

Research Article

The Coefficient of Tunnel Broken Zone and Field Test

Wei Guo, De-yi Jiang and Hua-fu Qiu

State Key Laboratory of Coal Mine Disaster Dynamics and Control,
Chongqing University, Chongqing 400044, China

Abstract: The coefficient of tunnel broken zone combined with the max thickness is used to describe the loosening zone distribution after excavation, which defined to the ratio of broken zone area to tunnel cross section. With 16 operation modes designed by Orthogonal test, coefficient of the broken zone can be obtained with numerical methods. The findings suggest that the order of each factor is: surrounding rock grades, ratio of depth to span, side pressure coefficient, buried depth, span length. Gonghe tunnel of Yu-Xiang highway is used to introduce the basic flow of tunnel broken zone coefficient test. Results show that the broken zone coefficient is closely related to geological conditions and excavation methods and the scope of broken zone can effectively reduce by selecting suitable ratio of depth to span and excavation method.

Keywords: Broken zone, excavation, field test, numerical methods, orthogonal test

INTRODUCTION

Influencing factors of tunnel loosening zone include three aspects, geological conditions, section structures and disturbance influence. The thickness of loosening zone is used to determine the size of loosening zone; however this index cannot fully reflect the distribution of loosening zone in the surrounding rock. Tunnel broken zone coefficient, the ratio of loosening zone area to tunnel cross section is introduced to evaluate the loosening zone.

Dong *et al.* (1991) analyzed the main influencing factors of loosening zone with physical simulation experiment; Xia (2009) studied the influence of depth (ground stress), mechanical parameters of rock (cohesion and internal friction angle) and ratio of depth to span; Sun (2006) analyzed the influencing of excavation cross-sectional area, height and span; Xiao *et al.* (2010) researched the influence of blasting on loosening zone based on the in-situ testing results. Five influencing factors (Liu and Song, 2003; Jing *et al.*, 1999; Zhao *et al.*, 2004), surrounding rock grades (Wang *et al.*, 2007), depth, span length, ratio of depth to span (Chen *et al.*, 2011) and side pressure coefficient are considered in this study, with 16 operation modes designed by orthogonal test (Fang and Changxin, 2001), thickness and coefficient of the loosen zone can be obtained by numerical methods (Wu, 2005). The importance degree of influencing factors is determined by Range analysis (Li *et al.*, 2004). In-situ testing of Gonghe tunnel in Chongqing China is used to introduce the general methods and processes of loosening zone coefficient field test.

In this study, the coefficient of tunnel broken zone combined with the max thickness is used to describe the loosening zone distribution after excavation, which defined to the ratio of broken zone area to tunnel cross section. With 16 operation modes designed by Orthogonal test, coefficient of the broken zone can be obtained with numerical methods. The findings suggest that the order of each factor is: surrounding rock grades, ratio of depth to span, side pressure coefficient, buried depth, span length. Gonghe tunnel of Yu-Xiang highway is used to introduce the basic flow of tunnel broken zone coefficient test. Results show that the broken zone coefficient is closely related to geological conditions and excavation methods and the scope of broken zone can effectively reduce by selecting suitable ratio of depth to span and excavation method.

COEFFICIENT OF BROKEN ZONE

Coefficient of broken zone (F_s), the ratio of loosening zone area (S_s) to tunnel cross section (S_d). At the assumption of the excavation section is circular (Fig. 1), radius equal to r_1 , the surrounding rock is isotropic and homogeneous rock and the horizontal stress is equal to vertical stress (the side pressure coefficient is 1); the radius of loosening zone is r_2 , thickness $R_s = r_2 - r_1$ and F_s is defined by Eq. (1) and (2):

$$F_s = \frac{S_s}{S_d} = \frac{\pi(r_2^2 - r_1^2)}{\pi r_1^2} = \frac{r_2^2 - r_1^2}{r_1^2} = \left(\frac{r_2}{r_1}\right)^2 - 1 \quad (1)$$

Corresponding Author: Wei Guo, State Key Laboratory of Coal Mine Disaster Dynamics and Control, Chongqing University, Chongqing 400044, China

This work is licensed under a Creative Commons Attribution 4.0 International License (URL: <http://creativecommons.org/licenses/by/4.0/>).

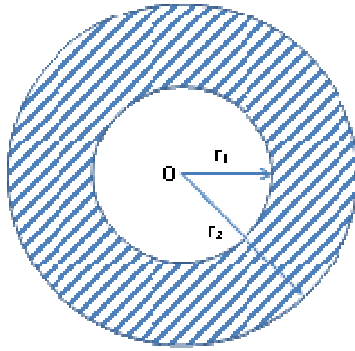


Fig. 1: Schematic diagram of loosening zone of tunnel

$$R_s = r_1 (\sqrt{F_s + 1} - 1) \quad (2)$$

Influencing factors of broken zone coefficient:

Mechanical parameters of rock: Compressive strength of rock mass is significantly larger than the tensile or shear strength, we usually just consider the influence of rock compressive strength. Based on mohr-coulomb criterion, the compressive strength of rock Eq. (3) can be defined with cohesion and internal friction angle. Research shows that the thickness of loosening zone is decreases with the increase of cohesion or internal friction angle:

$$\sigma_c = \frac{2C}{1 - \sin \phi} \quad (3)$$

Buried depth: Before excavation, surrounding rock is in equilibrium state under triaxial stresses. After excavation, if concentrated stress exceeds the surrounding rock strength, surrounding rock will break and reach a new equilibrium state of triaxial stresses in the deep. Due to that, the loosening zone is developed with the increase of buried depth and decreases with big strength. When the concentrated stress is less than its strength, the surrounding rock is in stable elasto-plastic state and no loosening zone exists.

Construction of tunnel section: The influence factors of tunnel section include excavation cross-sectional area, height and span, section shape. Study shows that the Loosening Zone increases with the excavation area; both sides of tunnel the loose areas will rapidly spread with the section height increases; with the excavation section span increases, the loosening zone become larger. As other section shape may cause unbalance distribution of stresses, three-centered circular are usually used.

Side pressure coefficient: The side pressure coefficient (S_2) is the ratio of horizontal stress to vertical stress. Measurement data at home and abroad shows that, the

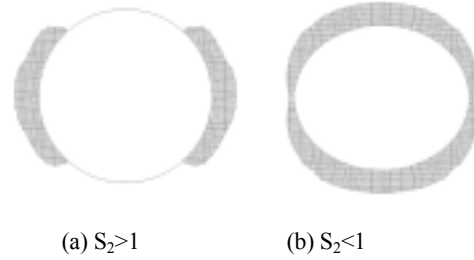


Fig. 2: The distribution of broken zone with different side pressure coefficient (S_2)

Table 1: Five factors and 4 level of test

Level	Factors				
	T	H (m)	D (m)	S_1	S_2
1	II	200	10	0.50	0.4
2	III	400	15	0.75	0.8
3	IV	600	20	1.00	1.2
4	V	800	25	1.25	1.6

T: Surrounding rock grades; H: Buried depth; D: Span length; S_1 : Ratio of depth to span; S_2 : Side pressure coefficient

Table 2: Physical and mechanical parameters of rock masses

Parameter	Rock grade			
	II	III	IV	V
Modulus of elasticity (GPa)	20.0	10.00	4.0	2.00
Poisson's ratio	0.2	0.25	0.3	0.35
Unit weight (KN/M ³)	26.0	24.00	21.0	18.00
Cohesion (MPa)	1.5	0.80	0.4	0.20
Angle of friction	50.0	40.00	35.0	27.00

horizontal stress is bigger than the vertical stress in common. The initial stress field of surrounding rock constitutes of two parts, gravity stress and tectonic stress. The change law of two stresses is different in nature, in some places the gravity stress is dominated, other places the tectonic stress become leading actor. The vertical stress and horizontal stress are increase with the increase of buried depth. The change of ground stress and geological structure lead to different side pressure coefficient. The distribution of broken zone with different side pressure coefficient is show in Fig. 2.

Analysis of influence factors:

Orthogonal test design: Five influencing factors, surrounding rock grades T, depth H, span length D, ratio of depth to span S_1 and side pressure coefficient S_2 are considered in this study. The orthogonal test design use 5 factors and 4 level to test L16 (4^5), we need to do 16 experiments, all factors and levels data are list in Table 1 and 2.

Numerical simulation: Use finite element software to simulation the 16 condition. The surrounding rock is isotropic and homogeneous, section shape is Three-centered circular (Fig. 3), the boundary of model is 5 times bigger than the span length of tunnel, failure

Table 3: Orthogonal experimental operation modes

No	Factors					Result	
	T	H (m)	D (m)	S ₁	S ₂	Rs (m)	Fs
1	II	200	10	0.50	0.4	2.4	0.22
2	II	400	15	0.75	0.8	0.0	0.00
3	II	600	20	1.00	1.2	0.0	0.00
4	II	800	25	1.25	1.6	0.0	0.00
5	III	200	15	1.00	1.6	0.0	0.00
6	III	400	10	1.25	1.2	0.0	0.00
7	III	600	25	0.50	0.8	2.7	0.06
8	III	800	20	0.75	0.4	4.6	0.40
9	IV	200	20	1.25	0.8	1.9	0.10
10	IV	400	25	1.00	0.4	4.9	0.39
11	IV	600	10	0.75	1.6	1.9	0.22
12	IV	800	15	0.50	1.2	1.9	0.53
13	V	200	25	0.75	1.2	8.2	0.97
14	V	400	20	0.50	1.6	8.5	1.72
15	V	600	15	1.25	0.4	7.3	1.24
16	V	800	10	1.00	0.8	2.9	1.12

Table 4: Range analysis of broken zone coefficient

Name	Factors				
	T	H (m)	D (m)	S ₁	S ₂
Average 1	0.055	0.323	0.389	0.634	0.560
Average 2	0.115	0.527	0.442	0.398	0.319
Average 3	0.309	0.379	0.555	0.376	0.377
Average 4	1.262	0.512	0.355	0.334	0.486
Range	1.207	0.204	0.200	0.300	0.241

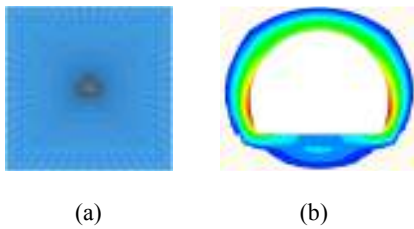


Fig. 3: Mesh diagrams for finite element models

criterion is DP. The mechanical parameters of rock are determined by the Code for Design of Road Tunnel (JTG D70-2004). Table 3 shows orthogonal experimental operation modes.

Range analysis: By orthogonal experiments and range analysis, surrounding rock grades T is the most important factor, following by ratio of depth to span S₁, side pressure coefficient S₂, depth H and span length D. Table 4 shows the range analysis of broken zone coefficient.

PRINCIPLE AND PROCESS OF TEST

Basic principle of test: Ground-Penetrating Radar (GPR) is a geophysical method that uses radar pulses to image the subsurface. This nondestructive method uses electromagnetic radiation in the microwave band (UHF/VHF frequencies) of the radio spectrum and detects the reflected signals from subsurface structures. GPR uses high-frequency (usually polarized) radio waves and transmits into the ground. When the wave hits a buried object or a boundary with different

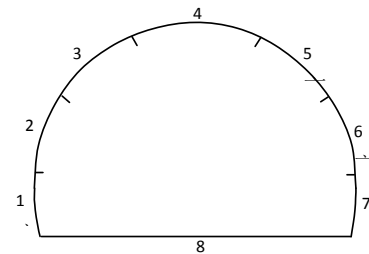


Fig. 4: Test line of section

dielectric constants, the receiving antenna records variations in the reflected return signal. The time of radio waves travel:

$$t = \sqrt{4h^2 + x^2} / v \tag{4}$$

- t = Travel time
- h = The depth of object
- x = The distance between transmitting and receiving antenna
- v = The speed of radio wave

Geotechnical and concrete are non-magnetic medium, in the frequency range of radar, the velocity of radio wave is:

$$v = \frac{c}{\sqrt{\xi}} \tag{5}$$

- C = Velocity of light
- ξ = Relative dielectric constant of medium

In the case that distances between transmitting and receiving antenna are much closed, the formula of depth of object is:

$$h = \frac{t}{2} \cdot v \tag{6}$$

Table 5: The section of measuring BRZ

Section mileage	Burial depth	Support pattern	Excavation method
ZK40+750	318 m	III (C)	Up and down step method
ZK41+095	448 m	III (C)	Up and down step method
ZK41+350	500 m	III (D)	Up and down step method
K41+350	500 m	III (D)	Full face excavation method

Table 6: The max thickness of broken zone at each section

Section mileage	ZK40+750	ZK41+095	ZK41+350	K41+350
Part 1	1.30	3	4.70	2.20
Part 2	1.50	3	5	2.20
Part 3	1.70	7	6	4
Part 4	2.20	7	8	5
Part 5	2.30	7.50	8	5
Part 6	2.10	5	6	5
Part 7	1.80	5	4.60	4
Fs	0.62	2.38	2.72	1.56

Detection process: In-situ testing can be divided into three stages:

- **Preparation stage:** Collect geological data of the test section and in-site monitoring data. Take three heart circle cross-section for example, shown in Fig. 4, typically section is divided into seven individual parts to test. According to the actual situation of field, 8th region of tunnel invert may be tested.
- **Detection stage:** Selects appropriate antenna frequency based on experience or pilot test results and then detects the section.
- **Analysis stage:** Obtains the max thickness and location of loosening zone with the test data and calculates the coefficient of loosening zone.

In-site test example:

Introduction: Gonghe tunnel locate in southeast of sichuan basin of china, west side of Darou mountain, belong to wujiang river gorge area with gully erosion. The length of left tunnel is 4745 m from ZK39+983 to ZK44+728; the right tunnel is 4779 m from K39+965 to K44+744.

In order to comparative analysis, four tunnel sections (Table 5) with different buried depth and excavation method were selected to detection.

Support pattern III (C): grouted rockbolt diameter is 0.022 m; length is 3.0 m; longitudinal space is 1.2 m; ring direction space is 1.0 m; grid steel frame (0.175×0.175 m, reinforcement diameter is 0.025 m), longitudinal space is 1.2 m; Support pattern III (D) has same parameters like III (C) but grid steel frame longitudinal space is 1.02 m.

Analysis conclusion: The GPR type SIR-20 produced by GSSI United States is used to field test. The result of field test list in Table 6, the section width is 12.3 m, side-wall height is 1.5 m.

Finally, our analysis with the test data showed that the coefficient of broken zone is highly correlated with support pattern, excavation method and so on. The details are list as below:

- The max thickness of loosening zone is area 4 and 5.
- The thickness and coefficient of broken zone is increase with buried depth. The loosening zone is suitable under 318 m depth and significantly increase when the buried depth increase to 450 m.
- Test shows that the thickness and coefficient of broken rock zone also influenced with excavation methods.

CONCLUSION

By orthogonal experiments and range analysis, surrounding rock grades T is the most important factor, following by ratio of depth to span S_1 , side pressure coefficient S_2 , depth H and span length D.

Ground-penetrating radar is used to field test, detection process can be divided into three stages: Preparation, Detection and analysis.

The test of Gonghe tunnel shows coefficient of broken zone is increase with buried depth and full-face excavation is better than bench method.

ACKNOWLEDGMENT

This study was financially supported by the National Key Basic Research Program (No. 2009CB724606) and Natural Science Foundation of China (51074198).

REFERENCES

- Chen, W., H. Wang and T. Hongming, 2011. Study of flat ratio optimization of large-span tunnel section in shallow broken rock mass. Chinese J. Rock Mech. Eng., 30(7): 1389-1395.
- Dong, F., G. Zhihong and L. Bing, 1991. The theory of supporting broken zone in surrounding rock [J]. J. China Univ. Min. Technol., 2(1): 64-71.
- Fang, K. and M. Changxin, 2001. Orthogonal and Uniform Experimental Design [M]. Science Press, Beijing.
- Jing, H., F. Guobin and G. Zhihong, 1999. Measurement and analysis of influential factors of broken zone of deep roadways and study on its control technique [J]. Chinese J. Rock Mech. Eng., 18(1): 70-74.
- Li, X., Z. Weishen, C. Weizhong and K. Wu, 2004. Determining weight of factors in stability analysis of underground caverns by analytic hierarchy process [J]. Chinese J. Rock Mech. Eng., 23(2): 4731-4734.
- Liu, G. and H. Song, 2003. Numerical simulation of factors affecting broken rock zone [J]. Min. Metallurg. Eng., 23(1): 1-3.

- Sun, Y., 2006. Influence of geometry on the broken zone of underground cavity [D]. MS Thesis, Institute of Engineering Mechanics, China Earthquake Administration, Harbin.
- Wang, S., H. Faliang and L. Changsong, 2007. Rock Classification in Tunnel Engineering [M]. Southwest Jiaotong University Press, Chengdu, China.
- Wu, R., 2005. The numerical simulation on highway tunnel stability and mechanical mechanism of tunnel single shell lining [D]. MS Thesis, Southwest Jiaotong University, Chengdu, China.
- Xia, F., 2009. The factors analysis of underground cavity broken zone [D]. MS Thesis, Institute of Engineering Mechanics, China Earthquake Administration, Harbin.
- Xiao, J., X. Fang and D. Lin, 2010. Influence of blasting round on excavation damaged zone of surrounding rock [J]. *Chinese J. Rock Mech. Eng.*, 29(11): 2248-2252.
- Zhao, X., J. Duan and T. Chun'an and Z. Wancheng, 2004. Study on failure mode of tunnels with different sections [J]. *Chinese J. Rock Mech. Eng.*, 23(2): 4921-4925.